Assiut University Journal of Chemistry (AUJC) 44(2015)13-26

Journal homepage: www.aujc.org

ISSN 1678-4919

Vol(44)	No(1)	2015

Full Paper

Spectral, Thermal ,Voltammetric and Biological Studies on Mn(Ii),Fe(II,III), Co(II), Cu(II) and Zn(II) With Cefazolin Antibiotic

Amna S.A. Zidan and Nagwa Abo El-Maali
Chemistry Department, Faculty of Science, Assiut University, Assiut, Egypt.
E-mail: amna.zidan@yahoo.com

Article history : Received:1/1/2015 ; Revised : 20/5/2015 ; Accepted : 23/5/2015; Available Online : 1/6/2015;

Abstract:
The following complexes of cefazolin(HCefaz) antibiotic were synthesized and investigated: $[M(Cefaz)_2].xH_2O$ where M=Mn(II),Co(II) ,Cu(II);x=0,4,2and $[M(Cefaz)_{y}.Cl.H_2O].xH_2O$ where M = Fe(II), Co(II), Zn(II); y = 1; x=0,3,2 and M = Fe(III); y = 2; x = 3 .The complexes have been characterized on the basis of elemental analyses, IR, electronic and mass spectroscopy. The thermal behavior of the complexes was followed by thermo gravimetric analysis (TG) and differential thermogravimetry (DTG). The IR spectra showed that the ligand acts in a mononegative bidentate fashion. Preliminary pharmacological tests on cefazolin salt and its complexes exhibited some antimicrobial activity.

1. INTRODUCTION

Cefazolin is one of the β-lactam antibiotics which have been known to behave as relatively efficient chelating agents[1]. They are the most important class of drugs against infection diseases caused by bacteria[2,3]. The biologically active principle of these antibiotics in the β-lactam ring, the reactivity and selectivity of which towards biological substrates can be decisively modified by substituent. Cefazolin is more active against E. coli and Klebsiella species[3]. Essential trace metal ions like zinc and copper are present in too low concentrations in blood plasma to significantly influence the bio-availability of these drugs[4,5]. However, the belief that antibiotic action is related to the ability of these compounds to form complexes with metal ions has simulated investigations of the complexion properties of antibiotics as ligands[6,7]. Investigation on the binary complexes of cefazolin may therefore help toward understanding the driving forces leading to the formation of such complexes in biological systems. We describe here the synthesis, spectral, thermal and voltammetric studies and antimicrobial activity tests of Mn(II),Fe(II,III), Co(II), Cu(II) and Zn(II) with cefazolin

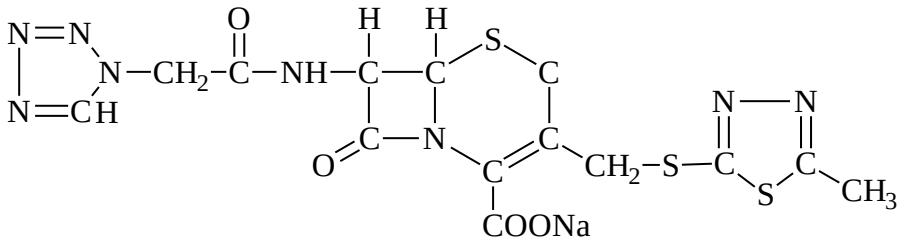

Fig. 1: Structure of cefazolin salt.

2. EXPERIMENTAL

All chemicals were of analytical grade. Cefazolin sodium salt was provided generously from Bristol-Myers Squibb Company Egypt.

2.1 Physical Measurements

Carbon, hydrogen, nitrogen and sulphur were determined by Analytisher Funklionstest Vario El-Fab-Nr. 11982027 apparatus. The IR spectra of the ligand and its metal complexes were made in KBr pellets on a 470 Shimadzu infrared spectrometer. The electronic spectra in dimethylformamide (DMF) were carried out on an UV-2101PC Shimadzu spectrophotometer at room temperature. FAB mass spectra were recorded at JEOL-JMS600 apparatus. Thermal analysis were measured on the TGAV5.IA Dupont 2000 apparatus.

2.2 Synthesis of the Complexes

The complexes were prepared by mixing the sodium salt of the cefazolin (1 mmol or 2 mmol) dissolved in the minimum amount of doublet distilled water (~10 mL) with 10 mL of an aqueous solution of 1 mmol metal chloride in the molar ratios metal : ligand 1:1 and 1:2 at room temperature. The solid complexes were precipitated after a time period ranging from ½ hr - 3 days. The complexes were filtered, washed with 1-2 ml of distilled water, 80% ethanol and diethyl ether, and finally dried by suction.

2.3 Antimicrobial Activity

The antimicrobial activity of the ligand (cefazolin salt) and all complexes against E. coli, B. cereus and P. aeruginosa were determined using Cup-diffusion method[8].

Each compound was dissolved in dimethyl-formamide with the a concentration of 500 $\mu g.mL^{-1}$.

2.4 Voltammetric measurements

Voltammetric measurements are recorded using the CV-50W Voltammetric Analyzer (USA) electrochemical running under windowsTM software. All controlled parameters are entered through a BAS/windows interface. This information is transferred to the CV-50W microprocessor where optimum hardware settings are calculated for the specified technique. These values are loaded automatically and upon applying the command run; data is collected and transmitted to the PC where it is displayed in virtual real time. Standard C-2 cell stand is fully shielded in a Faraday cage (EF-1080) with three electrodes: a glassy carbon working electrode (MF- 2012, diameter 3 mm), a silver/silver chloride reference electrode (MF- 2063) and a platinum wire auxiliary electrode (MW-1032). Voltammograms are collected using an hp HEWLETT PACKARD laser jet 4L printer. The pH's were measured using the Fisher Scientific Accument pH Meter Model 810 equipped with a combined glass electrode, which is calibrated regularly with buffer solutions (pH 4.00 and 7.00) at 25 ± 1°C. V3 series HTL micropipettes (Germany) were used to pipette µL volumes of solutions.

3. RESULTS AND DISCUSSION

The solid complexes of cefazolin can be readily obtained by mixing an aqueous solution of its sodium salt with the respective metal chloride of Mn(II), Fe(II), Fe(III), Co(II), Cu(II) or Zn(II). The resulting

complexes can be divided into two types according to their stoichiometric ratios, namely 1:2 and 1:1 (M:L). The following equations represent the preparation of the complexes:

$$2NaCefaz + MCl_2 + xH_2O \rightarrow [M(Cefaz)_2].xH_2O + 2NaCl$$

M = Mn(II), Co(II) , Cu(II); x = 0, 4,2,

$$yNaCefaz + MCln + xH_2O \rightarrow [M(Cefaz)_yCl.H_2O].xH_2O + yNaCl$$

M = Fe(II), Co(II) or Zn(II); n = 2; y =1; x = 0,3,2

and M=Fe(III); n=3; y=2; x=3

It is to be noted that even when the metal to ligand molar ratio 2:1 (M:L) was used, only complexes of the molar ratio 1:2 or 1:1 were isolated. The complexes are fairly soluble in DMF and DMSO, but sparingly soluble in water, alcohol, acetone and chloroform. Analytical data of the complexes are collected in Table 1.

Table 1: Physical and Analytical Data of the Complexes.

Compound	Colour	Elemental analysis Found (Calc.%)				dec. p
		C	H	N	S	°C
$[Mn(Cefz)_2]$	White	34.95 (34.89)	2.93 (2.92)	23.28 (23.25)	20.00 (19.96)	380
$[Fe(Cefz)_2Cl.H_2O].3H_2O$	Brown	31.42 (31.36)	3.62 (3.59)	20.95 (20.90)	18.00 (17.94)	300
$[Fe(Cefz)Cl.H_2O]$	Yellow	29.75 (29.82)	2.90 (2.86)	19.90 (19.87)	17.12 (17.06)	320
$[Co(Cefz)_2].4H_2O$	Pink	32.30 (32.34)	3.47 (3.49)	21.60 (21.55)	18.47 (18.50)	355
$(Co(Cefz)Cl.H_2O].3H_2O$	Pink	27.12 (27.08)	3.60 (3.57)	18.10 (18.05)	15.50 (15.49)	330
$[Cu(Cefz)_2].2H_2O$	Green	33.40 (33.34)	2.98 (3.02)	22.25 (22.22)	19.10 (19.07)	335
$[Zn(Cefz)Cl.H_2O].2H_2O$	Pale yellow	27.65 (27.59)	3.35 (3.31)	18.45 (18.39)	15.75 (15.79)	315

3.1 IR Spectra

The IR spectral data of the ligand and the complexes are recorded in Table 2. Tentative assignments have been made on the basis of earlier publications and important bands are assigned as follows:

i) The IR stretching frequencies of the carboxylate group are very important for determining the structure of the complexes, when there are interactions between the carbonyl oxygen atoms of the carboxylate groups and the metal ion. The difference between asymmetric $\upsilon_{as}(CO_2^-)$ and symmetric $\upsilon_s(CO_2^-)$ vibration frequencies is related to the mode of coordination of the carboxylate group. So, the monodentate behavior of CO_2^- group in our complexes is suggested, where the difference between $\upsilon_{as}(CO_2^-)$ and $\upsilon_s(CO_2^-)$ occurs in the range 200-215 cm^{-1}. This range was reported for similar complexes[9,10].

ii) A shift in the frequency is also recorded for $\upsilon_{(NC)}$ (1460-1480 cm^{-1}) if compared to that of the ligand (1490 cm^{-1}). This may be due to coordination through the nitrogen atom adjacent to the carboxyl group. The strong bands appearing at 1680 and 1540 cm^{-1} in the ligand and corresponding to stretching vibrations of amide(I) and amide(II) are red shift upon complex formation[11] to 1660-1675 cm^{-1} and 1525-1535 cm^{-1}, respectively.

iii) Further, $\upsilon_{(NH)}$ and $\upsilon_{(OH)(H_2O)}$ are assigned to the bands located in range 3280-3310 and 3400-3450 cm^{-1}, respectively.

Table 2: Infrared Spectral Data for Cefazolin Salt and Complexes (cm^{-1}).

Compound	υ(NH) + υ(OH) (H_2O)	$\upsilon_{as}(CO_2^-)$	$\upsilon_s(CO_2^-)$	$\Delta\upsilon$	υ(NC)	Amide I	Amide II
Cefaz salt	3300, --	1600	1390	210	1490	1680	1540
$[Mn(Cefaz)_2]$	3300, --	1580	1370	210	1475	1670	1530
$[Fe(Cefaz)_2Cl.H_2O]3H_2O$	3310, 3410 br	1585	1370	215	1480	1675	1535
$[Fe(Cefaz)Cl.H_2O]$	3300, 3400	1590	1375	215	1480	1675	1535
$[Co(Cefaz)_2].4H_2O$	3305, 3410 br	1590	1380	210	1475	1670	1530
$(Co(Cefaz)Cl.H_2O].3H_2O$	3310, 3400	1580	1370	210	1470	1670	1530
$[Cu(Cefaz)_2].2H_2O$	3290, 3450	1570	1370	200	1465	1660	1525
$[Zn(Cefaz)Cl.H_2O].2H_2O$	3280, 3430	1575	1365	210	1460	1665	1530

3.2 Electronic Spectra

The electronic spectral data of the complexes and the ligand are recorded in DMF solvent and given in Table 3. From the data it is to be noted that the complexes display a number of bands in the UV-Vis region.

All complexes and ligand show highest energy bands in two regions 30,211-35,842 cm^{-1} and 36,232-46,948 cm^{-1} attributed to intraligand charge transfer and π-π*[9] transitions. The d-d transitions are discussed in each metal ion as follows:

i) $[Mn(Cefaz)_2]$ exhibits d-d transition bands at 17,421 and 18,797 cm^{-1} assigned to the $^6A1g \rightarrow {}^4T1g$ transition for a tetrahedral geometry around Mn(II)[12].

ii) The complex $[Fe(Cefaz)_2Cl.H_2O].3H_2O$ shows two d-d transition bands at 12,469 and 14,469 cm^{-1} corresponding to $^6A_1 \rightarrow {}^4T_2(G)$ and $^6A_1 \rightarrow {}^4A_1$, $^4E(G)$, transition, suggesting an octahedral arrangement around Fe(III) ion[13,14]. The electronic spectrum of Fe(II) shows two weak intensity bands at 11,876 and 12,285 cm^{-1} corresponding to the transition $^2B_{2g} \rightarrow {}^2B_{1u}$ in an octahedral geometry around Fe(II) ion[15].

iii) The complexes $[Co(Cefaz)_2].4H2O$ and $[Co(Cefaz)Cl.H_2O].2H_2O$ display a d-d transition band in the range 11,299-14,327 cm^{-1}, assigned to the $^4A_2 \rightarrow {}^4T_1(p)$ transition characteristic of a tetrahedral geometry around Co(II)[16,17].

iv) The electronic spectrum of $[Cu(Cefaz)_2].2H_2O$ was characterized by a broad band centered at 11,875 and 12,285 cm^{-1} which may be due to a combination of the $^2B_{1g} \rightarrow {}^2A_{1g}$ and $^2B_{2g} \rightarrow {}^2E_g$ transitions in a square planar configuration of the complex[14,18].

v) The Zn(II) complex, $[Zn(Cefaz)Cl.H_2O].2H_2O$ shows a d^{10} character, where the stereochemistry of its complex can not be determined from UV and visible spectra. However, from the comparison between the complex and complexes of similar environment around Zn(II), a tetrahedral geometry is assumed for the new complex[19-21].

Table 3: Electronic Spectral Data for the Lignad and the Complexes (in DMF).

Compound	λmax (cm^{-1})
Cefz salt	32,910; 41.666; 46,948
$[Mn(Cefz)_2]$	17.421; 18,797; 28,090; 33,113; 36,630; 43,478
$[Fe(Cefz)_2Cl.H_2O].3H_2O$	12.468; 14,327; 30,211; 35,842; 38,910
$[Fe(Cefz)Cl.H_2O]$	11.876; 12,285; 35,460
$[Co(Cefz)_2].4H_2O$	11,299; 32,786; 39,370; 44,248
$(Co(Cefz)Cl.H_2O].3H_2O$	11,806; 12.468; 14,327; 30,211; 36,232; 38,911
$[Cu(Cefz)_2].2H_2O$	11,875; 12,285; 31,949; 42,017; 45,249
$[Zn(Cefz)Cl.H_2O].2H_2O$	28,986; 32,787; 44,643

3.3 Thermal Analysis

The TG thermogram of [Mn(Cefaz)$_2$], Fig.2 exhibits three decomposition steps with DTG maxima at 264, 338 and 527°C, respectively. The first step represents a mass loss in agreement with [Cefaz] which may abstract H$^\bullet$ to form a cefazolin molecule (calc. 47.15%; found 45.81%). The rest of the unstable complex (I) loses two radicals $C_2H_3N_4^\bullet$ + $C_3H_3S_2N_2^\bullet$ at the second step which in turn may take 2H$^\bullet$ forming two the molecules $C_2H_4N_4$ and $C_3H_4S_2N_2$ (calc. 22.25%; found 20.27%). The left unstable complex (II) decomposes forming MnS as the final product (calc. 9.05%; found 9.38%). The thermal decomposition may be represented as follows:

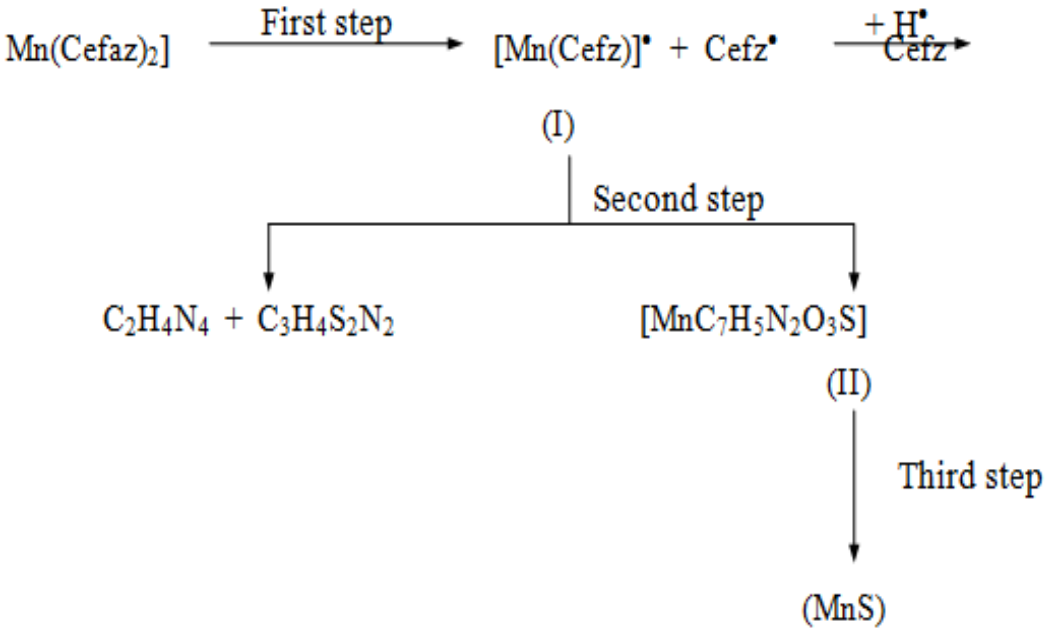

The TG and DTG thermograms of [Fe(Cefaz)$_2$.Cl.H$_2$O].3H$_2$O show three decomposition steps. The first step in the TG thermogram is associated with the expulsion of three water molecules. Their temperature range (~60°C) is typical for water of crystallization (calc. 5.05%; found 5.45%). The rupture at  takes place in the second step, leading to the formation of two radicals of (III) at 150-250°C which may abstract 2H$^\bullet$ to form two molecules of (IV) (calc. 20.74%; found 22.52%) before they decomposes. At the third step, two molecules of $C_4H_6S_2N_2$ and one water molecule were eliminated (calc. 30.46%; found 30.13%) in the temperature range 250-400°C. The final product is Fe_2S_3 (calc. 10.25%; found 9.20%).

The proposed thermal decomposition mechanism is:

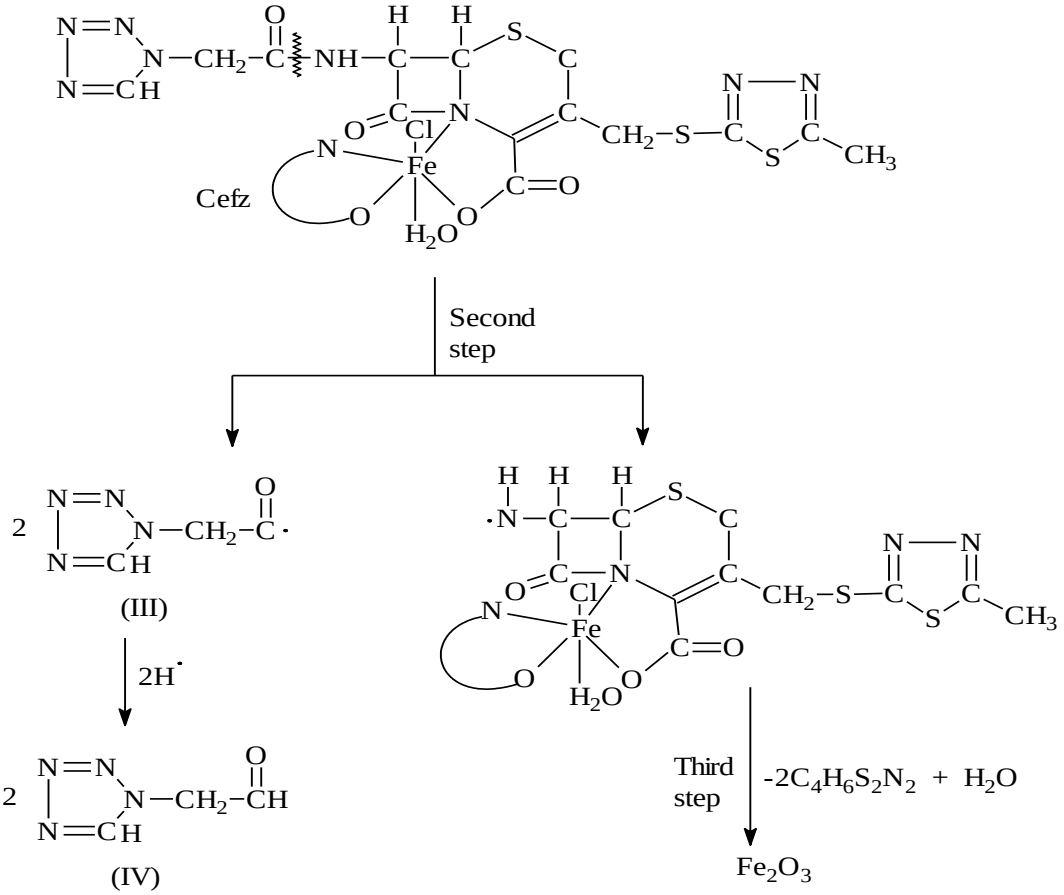

The pyrolysis curves of $[Co(Cefaz)_2].4H_2O$ and $[Co(Cefaz)Cl.H_2O].3H_2O$ exhibit three decomposition steps for each complex, namely at 35-170, 170-240 and 240-450°C and 35-170, 170-260 and 260-275°C respectively. The first stage in each DTG curve represents a mass loss of four water molecules (calc. 6.94%; found 7.25%) in the first complex and three water molecules in the second complex (calc. 8.72%; found 9.92%). The anhydrous complex $[Co(Cefaz)_2]$ decomposes in the subsequent two steps giving CoS as the final product (calc. 8.99%; found 9.65%) in the first complex. For the second complex, the step at 243°C (DTG curve) corresponds to the rupture in bond with the expulsion of a $[C_2H_3N_4]^{\bullet}$ radical which may take $H^{\bullet}$ to form V (calc. 13.40%; found 14.55%). This rupture was reported for similar complexes(22). The end product after complete decomposition is CoS (calc. 14.54%; found 13.02%).

The TG and DTG thermograms of $[Cu(Cefaz)_2].2H_2O$, Fig.3 show three decomposition steps (Table 4). The mass loss at the first step is in agreement with the elimination of two water molecules (calc. 3.58%; found 3.33%) at 80°C (DTG curve); this indicates that the water molecules are bonded in the crystal lattice. The mass loss in the second step at 215°C (DTG) is in agreement with the elimination of two radicals of $[C_4H_5S_2N_2]$ which may abstract $2H^{\bullet}$ giving (VI) or dimerize to form (VII) (calc. 28.84%; found 31.11%). The mass loss at 321°C (calc. 22.10%; found 25.03%) may be due to the release of $C_2H_4N_4O$ molecule. The end product was CuS (calc. 9.50%; found 9.63%). The decomposition behavior of $[Zn(Cefaz)Cl.H_2O].2H_2O$ is similar to that observed for $[Co(Cefaz)Cl.H_2O].2H_2O$ complex, where the first step represents a loss of two water molecules at 59°C (DTG curve) (calc. 5.30%; found 5.04%) and at 237°C; the

C_2H_3N4 molecule was eliminated (calc. 12.22%; found 13.35%). The rest of the unstable complex decomposes in the third step forming ZnS as the final product (calc. 16.03%; found 17.00%). The decomposition mechanism for this process is virtually similar to that in [Co(Cefaz)Cl.H2O].

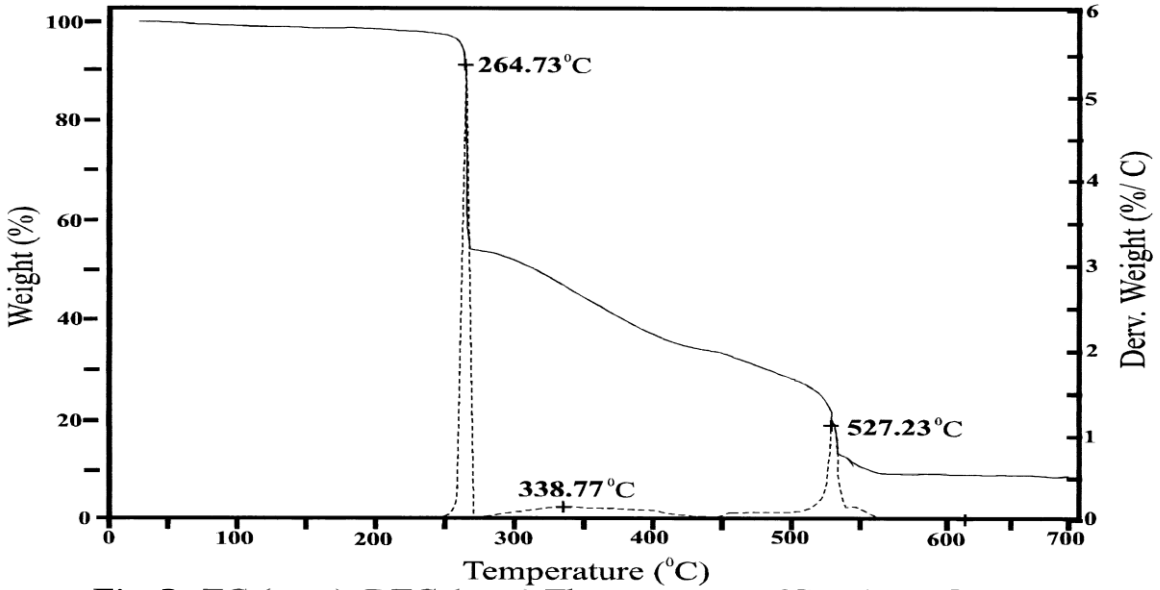

Fig. 2: TG (——), DTG (------) Thermograms of [Mn(Cefz)$_2$].

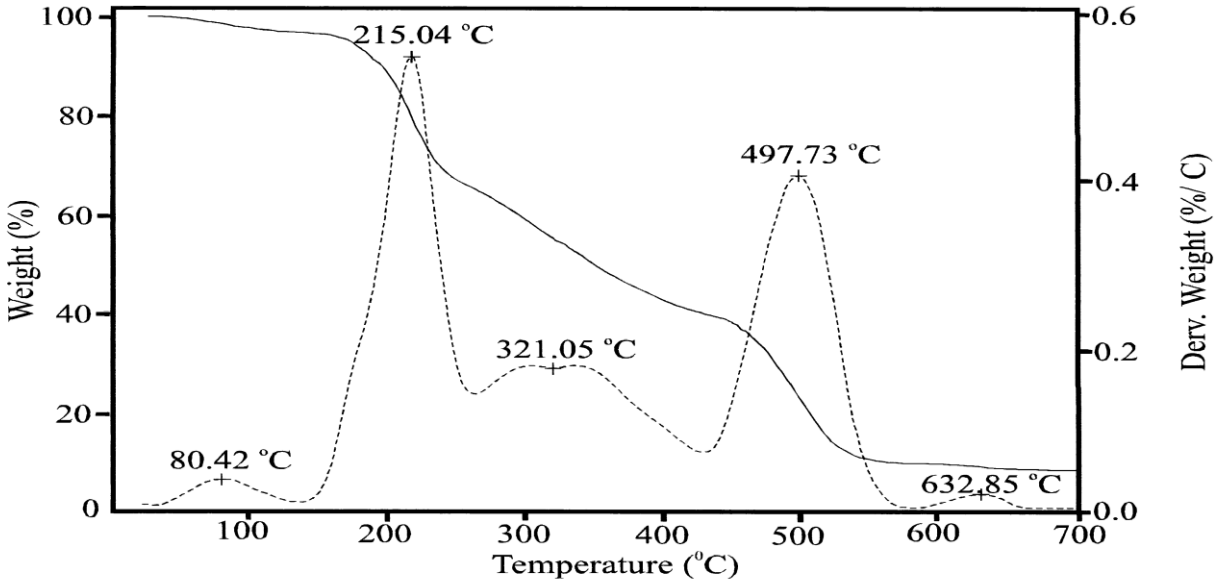

Fig. 3: TG (——), DTG (------) Thermograms of [Cu(Cefz)$_2$].2H$_2$O

Table 4: TG and DTG Data of the Complexes.

Compound	Step	Temp. range, °C	Max. temp. °C	Mass loss % Found (calc.)
$[Mn(Cefz)_2]$	First	35-270	264	45.81 (47.15)
	Second	270-445	338	20.27 (22.25)
	residue		527	9.38 (9.04)
$[Fe(Cefz)_2Cl.H_2O].3H_2O$	First	35-150	60	5.45 (5.05)
	Second	150-250	221	22.52 (20.76)
	Third	250-400	288	30.13 (30.46)
	residue		445	9.20 (10.25)
$[Co(Cefz)_2].4H_2O$	First	35-170	70	7.25 (6.94)
	Second	170-240	225	30.75 (27.97)
	Third	240-450	338	24.59 (21.42)
	residue		518	9.65 (8.99)
$[Co(Cefz)_2Cl.H_2O].3H_2O$	First	35-170	67	9.92 (8.72)
	Second	170-260	243	14.55 (13.40)
	Third	260-475	279	32.98
	residue	-	506	13.02 (14.54)
$[Cu(Cefz)_2].2H_2O$	First	35-150	80	3.33 (3.58)
	Second	150-260	215	31.11 (28.84)
	Third	260-440	321	25.03 (22.10)
	residue		497	9.63 (9.50)
$[Zn(Cefz)Cl.H_2O].2H_2O$	First	35-145	59	5.04 (5.30)
	Second	145-275	237	13.35 (12.22)
	Third	275-440	325	34.05
	residue		577	17.00 (16.03)

3.4 Mass Spectra

The observed molecular ion peak [M+] in the mass spectrum of the Mn(II) complex suggests the proposed formula $[Mn(Cefaz)_2]$. Assignments of the mass spectral peaks indicate the presence of fragments corresponding to $[Cefz]^{\bullet+}$ and some complex species such as $[MnC_{22}H_{22}N_{12}O_8S_4]^{\bullet+}$ m/z 761 (7.6%), $[MnC_{19}H_{20}N_8O_7S_4]^{\bullet+}$ m/z 649 (6.7%), $[MnC_8H_9N_2O_3S_2]^{\bullet+}$ m/z 299 (5.3%) and $[MnC_6H_5N_2O_2S]^{\bullet+}$ m/z 209 (15%).

The mass spectrum fragments for $[Co(Cefz)_2].4H_2O$ were recorded in Scheme 1. The two radical ions of $[Cefz]^{\bullet+}$ and $[Co(Cefz)]^{\bullet+}$ were detected at m/z 454 and 512, respectively. The fragments of $[Cefz]^{\bullet+}$ were detected as well.

Scheme1

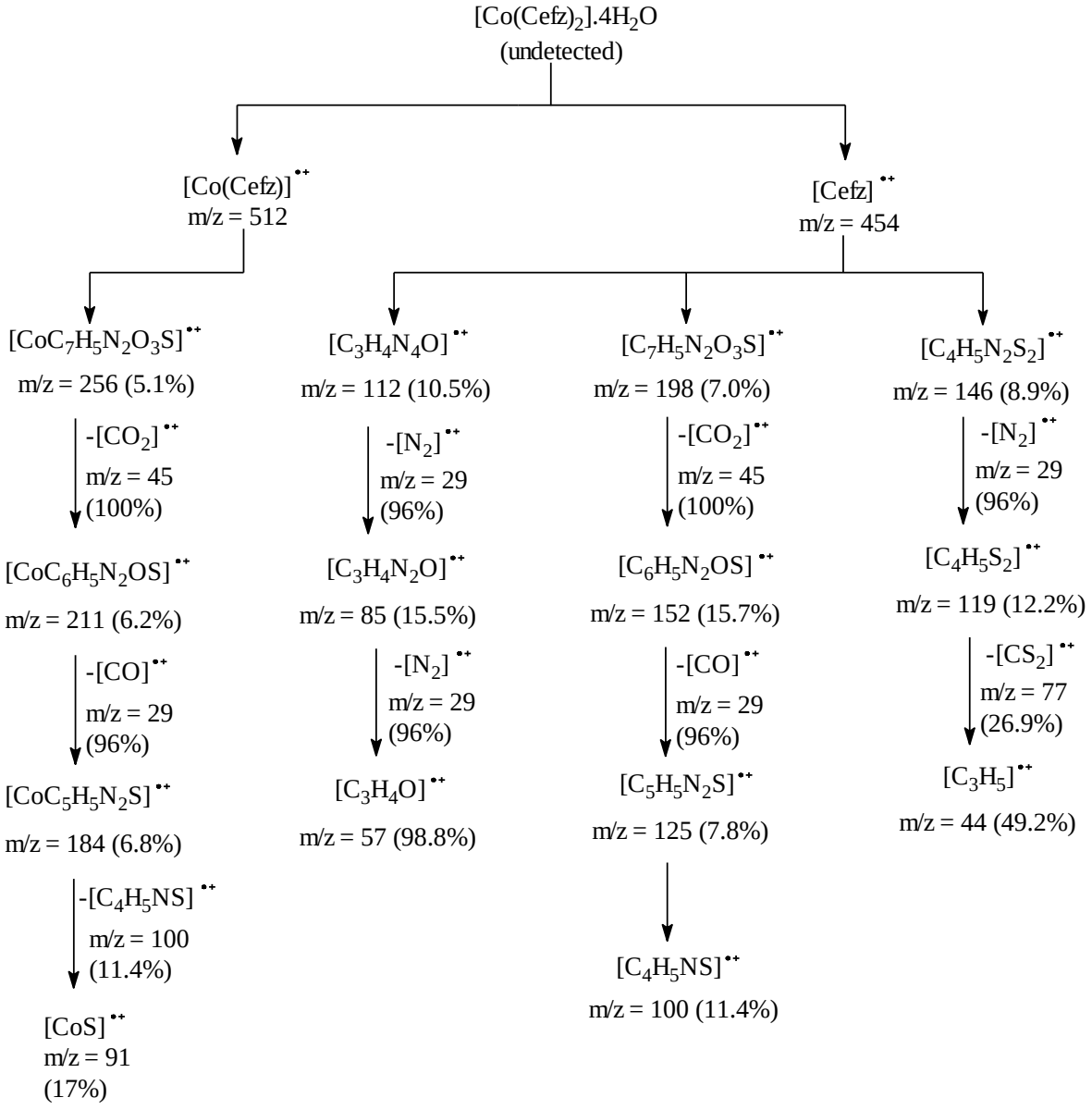

3.5 Voltammetric Studies

As voltammetry is a powerful tool for studying and elucidating a new structure, in this paper we have utilized voltammetry for studying the electrochemical behavior of cefazolin and its mentioned prepared solid complexes. For this purpose, osteryoung square wave voltammetry (OSWV) at the glassy carbon electrode has been applied using 0.1 M phosphate buffer solution adjusted to pH 5.95. Fig. 4 represents the OSWV of cefazolin (curve a) and that for the dissolved in DMSO- (curve b). Evidence of the complex formation is elucidated as a result of the appearance of the new peak at~ -1.35 V vs Ag/AgCl. $KCl_{(s)}$. This peak was attributed to the complex formation reaction with the proposed structure $[Mn(Cefz)_2]$.When a solution for the prepared iron complexes $[Fe(Cefaz)_2Cl.H_2O].3H_2O$ and$[Fe(Cefaz)Cl.H_2O]$ are separately introduced for the electrochemical cell -under the same experimental conditions-mentioned above, a little shift in the peak potential of

prepared manganese solid complex[$Mn(Cefz)_2$]- (curve b) for the [$Fe(Cefaz)Cl.H_2O$] complex whereas in addition to this shift an appearance of a shoulder (combined to the main peak) , curve c is obtained for the [$Fe(Cefaz)_2Cl.H_2O$].$3H_2O$ indicating different structures for both structures. For cobalt prepared solid complex beside the OSWV, cyclic votammetry (CV) has been also applied Fig.6, shows a shift in the peak potential of cefazolin (curve a) towards more negative potential together with the appearance of two new peaks at ~ -0.75 V and cefazolin (Fig 5, curve a) is observed -0.5 V in the cathodic side followed by a large oxidation peak at about –0.3 V in the anodic side which is probably due to the reduction of the cobalt metal ion in the complex structure. However, the appearance of these new peaks relies that the complex formation reaction involves changes in the orbitals of the ligand (cefazolin). For both Zinc and copper complexes, a shift in the peak potential of the ligand towards more negative potentials was also attributed to the complex formation reaction. Fig.7 shows the voltammograms recorded for cefazolin (curve a) and that for the [$Zn(Cefaz)Cl.H_2O$].$2H_2O$ prepared solid complex.

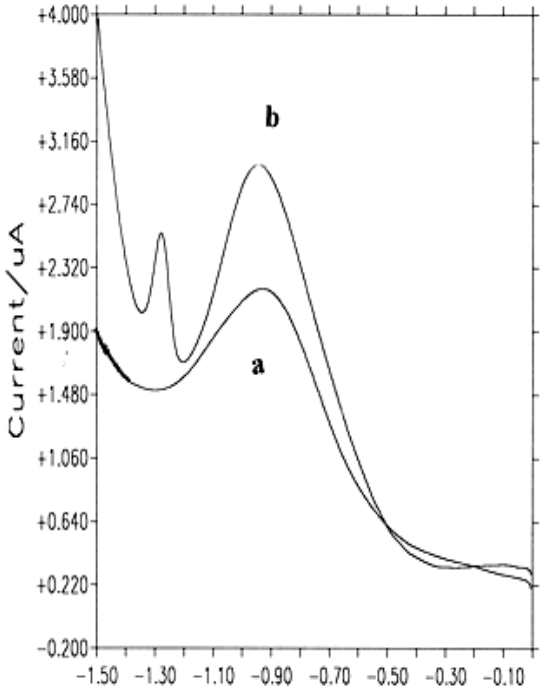

Fig. 4

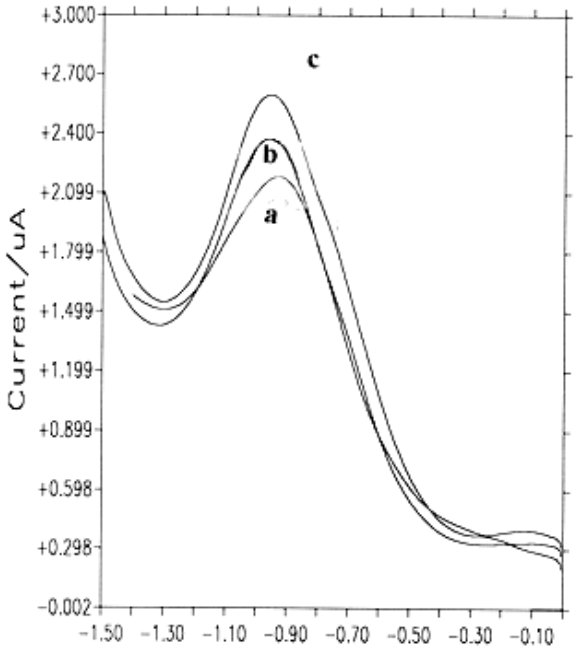

Fig. 5

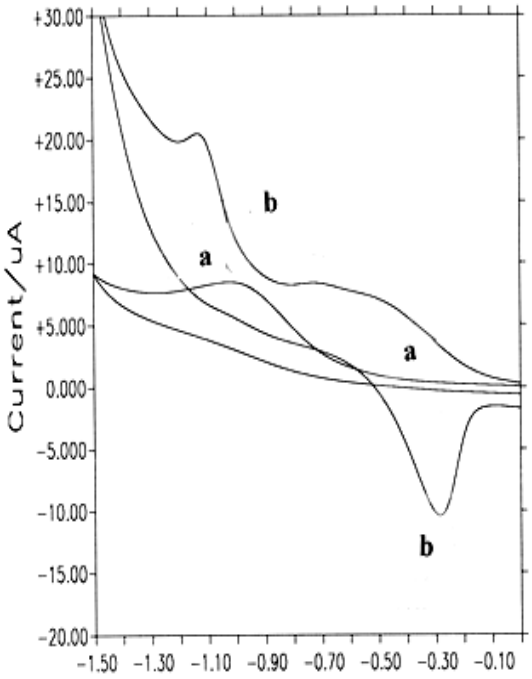

Fig. 6

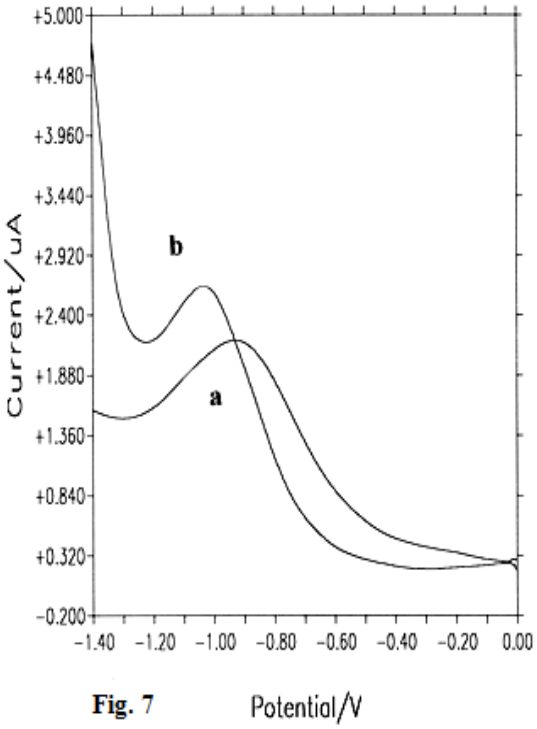

Fig. 7

3.6 Biological Activity

From the antibacterial data of Table 5, the antibacterial activity of the complexes can be divided to two classes comparable according to the activity of cefazolin salt drug.

a) The first class which showed significantly enhanced antibacterial activity against one or more bacterial species in comparison to the free ligand, involving $[Fe(Cefaz)_2Cl.H_2O].3H_2O$, $[Co(Cefaz)_2].4H_2O$, $[Cu(Cefaz)_2].2H_2O$ and $[Zn(Cefaz)Cl.H2O].2H_2O$ complexes.

i) It is clear that Fe(III) plays an important role in the antibacterial activity, where it shows higher activity against three bacteria, comparable to that of the other complexes and Cefaz salt. This may be due to two reasons: firstly, the chelating tends to make the ligand (Cefaz)− acts as more powerful and potent bactericidal agents, thus killing more of the bacteria than the Cefaz salt does[21]. The second reason is the increase in positive charge of the metal ion (Fe^{+3}) is partially shared with the donor atoms and there is π-electron delocalization over the role chelate positions. This increases the lipophilic character of the metal chelate and favors its permeation through lipid layers of the bacteria membranes[23-27].

b) The second class represents the inactive complexes against all bacterial species compared with Cefaz salt namely, $Mn(Cefaz)_2$, $[Fe(Cefaz)Cl.H_2O]$ and $[Co(Cefaz)Cl.H_2O].3H_2O$.

Table 5: Antibacterial Activity Data of Cefazolin and its Metal Complexes.

Compound	*B. cereus* (G +ve)	*E. coli* (G -ve)	*P. aeruginosa* (G-ve)
Cefaz salt	+	+	+
$[Mn(Cefaz)_2]$	-ve	-ve	-ve
$[Fe(Cefaz)_2Cl.H_2O].3H_2O$	+++	+++	+++
$[Fe(Cefaz)Cl.H_2O]$	-ve	-ve	-ve
$[Co(Cefaz)_2].4H_2O$	+++	++	+
$(Co(Cefaz)Cl.H_2O].3H_2O$	-ve	-ve	-ve
$[Cu(Cefaz)_2].2H_2O$	++	++	-ve
$[Zn(Cefaz)Cl.H_2O].2H_2O$	++	-ve	++

4. Conclusion

We could successfully prepare a number of metal complexes of the antibiotic cefazolin. The complexes we fully characterized by spectral and thermal studies. The complexes reveal relatively high thermal stability. Some of these compounds proved to be effective against a number of bacterial strains. The antibacterial action of most of them(especially those of iron complexes) is higher than the cefazoline itself indicating that the prepared compounds may have promising potential antibacterial activity.

References

[1] A .Albert, Nature 172 (1953) 201.

[2] A.Zaki, E.C Schreiber, I. Weliky, J.R Knill,J.A. Hubsher, J. Clin. Pharmacol. 14 (1974) 118.

Chemotherapy 18(1973) 191.

[4] w.A.Baker,P.N. Brown, J. Am. Chem. Soc.88 (1966) 1314.

[5] L.A.Mitscher ,A.C. Bonacci, B.Slater-Eng,A.K Hacher ,T.D. Sokoloski , Agents Chemother. p. III(1969)9.

[6] D.C.Ress, J. Mol. Biol.141 (1980) 323.

[7] N.K.Rogers ,G.R. Moore ,M.J.E. Stemberg, J. Mol. Biol.182 (1985) 613.

[8] Y.Tsukamoto ,K. Sato,K. K.Tanaka,T. Yanai , Bioscience Biotech. Biochem.61 (1997) 304.

[9] K. Nakamato , Infrared and Raman Spectra of Inorganic and Coordination Compounds, 3rd, Edn, Wiley, New York, (1978)232.

[10] G.Wang . Synth. React. Inorg. Met-Org. Chem.30 (2000) 601.

[11] M.M.Shoukry,A.K. Abdel Hadi,W.M.

[3] J. Klostersky,D. Danean ,D. Weerts , Hosny, Synth. React. Inorg. Met-Org. Chem.25 (1995) 45.
[12] D.Nickolls "Complexes and First-Raw Transition Elements", Macmillan, Great Britain (1974) 97.
[13] S.Vats ,L.M. Sharma, Synth. React. Inorg. Met-Org. Chem. 27(1997) 1565.
[14]A.B.P.Lever, "Inorganic Electronic Spectroscopy", Elsevier, Amsterdam (1968).
[15] G.M.Abou El-Reach , Synth. React. Inorg. Met-Org. Chem.23 (1993) 825.
[16] M.Schwartz ,W.E. Hatfield, Inorg. Chem.26 (1987)2823.
[17]N.K.Sing,S.B.Sing, Synth. React. Inorg. Met-Org. Chem.32 (2002) 25.
[18]A.B.P.Lever "Inorganic Electronic Spectroscopy", Elsevier, Amsterdam (1984).
[19]W.M Hosny, Synth. React. Inorg. Met-Org. Chem.27 (1997) 197.
[20] S.Chandra,L Gupta , Synth. React. Inorg. Met-Org. Chem.26 (1996) 125.
[21]M.Tümer,H. Koksal,S. Serin ,S. Patat, Synth. React. Inorg. Met-Org. Chem.27 (1997) 59.
[22] A.H.Oman,, N. Abo El-Maali, A. A.M.Aly, G. A.A. Al-Hazmi. Synth. React. Inorg. Met-Org. Chem.32 (2002) 763.

[23] W. Li, W.Long, R. Zuozuo, Z. Feng, J. Qiufang, L. Jun, J. of Shanxi Medical University,9 (2010) 804.

[24] Z.H.Chohan,A. Munawar,C.T Supuran , Metal-Based Drugs. 8(2001)137.

[25]Z.H.Chohan ,S. Kausar. Chem. Pharm. Bull.40 (1992) 2555.

[26]Z.H.Chohan ,M. Jaffery ,C.T Supuran , Metal-Based Drugs.8 (2001)95.

[27] M.Ul-Hassan,Z.H. Chohan,C.T. Supuran, Synth. React. Inorg. Met-Org. Chem.32 (2002) 529.